

General Disclaimer

One or more of the Following Statements may affect this Document

- This document has been reproduced from the best copy furnished by the organizational source. It is being released in the interest of making available as much information as possible.
- This document may contain data, which exceeds the sheet parameters. It was furnished in this condition by the organizational source and is the best copy available.
- This document may contain tone-on-tone or color graphs, charts and/or pictures, which have been reproduced in black and white.
- This document is paginated as submitted by the original source.
- Portions of this document are not fully legible due to the historical nature of some of the material. However, it is the best reproduction available from the original submission.



NATIONAL AERONAUTICS AND SPACE ADMINISTRATION

INTERNAL NOTE MSC - EG - 69 - 15

PROJECT APOLLO

COMPUTER SIMULATION
FLIGHT ACCELERATION FACILITY ENTRY MONITORING
SYSTEM STUDY



HYBRID COMPUTATION AND SIMULATION BRANCH
GUIDANCE AND CONTROL DIVISION

MANNED SPACECRAFT CENTER

HOUSTON, TEXAS

March 19, 1969

FACILITY FORM 602

N70-34659
(ACCESSION NUMBER)

(PAGES)

TMX 64364
(NASA CR OR TMX OR AD NUMBER)

(THRU)

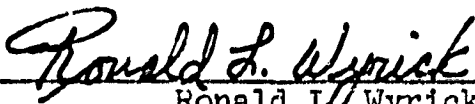
(CODE)

31
(CATEGORY)

PROJECT APOLLO

COMPUTER SIMULATION
FLIGHT ACCELERATION FACILITY ENTRY MONITORING SYSTEM STUDY

PREPARED BY

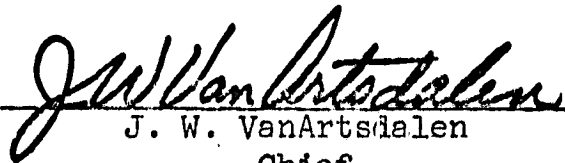


Ronald L. Wyrick

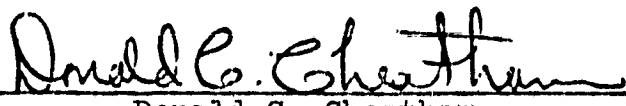


Walter R. Russell


APPROVED BY



J. W. VanArtsdalen
Chief
Hybrid Computation and Simulation Branch



Donald C. Cheatham
Assistant Chief
Guidance and Control Division



Robert G. Chilton
Deputy Chief
Guidance and Control Division

NATIONAL AERONAUTICS AND SPACE ADMINISTRATION
MANNED SPACECRAFT CENTER
Houston, Texas

March 19, 1969

COMPUTER SIMULATION
FLIGHT ACCELERATION FACILITY ENTRY MONITORING SYSTEM STUDY

INTRODUCTION

The Engineering and Development Directorate was asked to support the Flight Crew Operations Directorate in a closed loop Apollo entry simulation using the Flight Acceleration Facility (centrifuge). The objective of the simulation was to provide the flight crew a real time simulation to use the entry monitor system for lunar return entry conditions while subjecting the crew to realistic accelerations. At the time of the request, the flight acceleration facility of the Crew Systems Division did not have the computing capacity for a simulation of this size and the Guidance and Control Division was asked to aid in the work. The result was a joint effort of the Crew Systems Division and the Guidance and Control Division with the Crew Systems Division having overall responsibility for the job as well as supplying the centrifuge and the normal complement of supporting personnel and equipment. The Guidance and Control Division supplied the equations of motion, two analog computers, and programmed and operated the analog computers. The size of the task was such that the third computer had to be borrowed from the Computation and Analysis Division. Within the Guidance and Control Division, the Control Requirements Branch developed the vehicle equations of motion and aided in the checkout of the simulation. The Hybrid Computation and Simulation Branch programmed the equations, checked the simulation, and maintained the computers.

The purpose of this paper is to describe the analog simulation of the EMS equations of motion and how it interfaced with the overall system. The operation of the centrifuge and the programming of the centrifuge control computers will not be discussed in any detail.

SYMBOLS

A_x, A_y, A_z	Applied acceleration along $X_b, Y_b,$ and $Z_b,$ g's
a_x, a_y, a_z	Applied acceleration along $X_b, Y_b,$ and $Z_b,$ ft/sec ²
C_A, C_N, C_m	Aerodynamic axial and normal force coefficients and pitching moment coefficient, respectively
$C_{A_\eta}, C_{N_\eta}, C_{m_\eta}$	Slopes of aerodynamic $C_A, C_N,$ and C_m versus cosine η curve, respectively.
D	Spacecraft reference length, ft
g	Acceleration due to gravity, ft/sec ²
h, \dot{h}	Spacecraft altitude above sea level and altitude rate, ft, and ft/sec., respectively
I_x, I_y, I_z	Moment of inertia about $X_b, Y_b,$ and Z_b axes respectively, slug-ft ²
K_1	Gravitational gain factor
K_2, K_3, K_4	Ordinate value of C_A, C_N, C_m versus cosine η curve, respectively.
L_j, M_j, N_j	RCS jet rolling, pitching, and yawing moments, respectively, ft-lb.
m	Spacecraft mass, slugs
$\dot{P}, \dot{Q}, \dot{R}$ P, \dot{Q}, \dot{R}	Roll, pitch, and yaw rates and accelerations about $X_b, Y_b,$ and $Z_b,$ respectively, deg/sec and deg/sec ²
\bar{q}	Dynamic pressure, lb/ft ²
R	Reference radius of the earth, ft

S	Spacecraft reference area, ft^2
u, v, w	Body components of inertial velocity, ft/sec
$\dot{u}, \dot{v}, \dot{w}$	Components of body acceleration, ft/sec^2
V_T	Total velocity, ft/sec
Z_{cg}	Distance from spacecraft center line to c.g. along
	Z_b
$\tan \alpha_t$	Tangent of trim angle of attack (SCS)
$\tan \alpha_A$	Tangent of trim angle of attack (aero)
Cosine η	Cosine of total angle of attack
θ, ψ, ϕ $\dot{\theta}, \dot{\psi}, \dot{\phi}$	Euler angles and Euler angle rates, respectively, deg and deg/sec
ρ	Atmospheric density, slug/ft^3
ϕ_b	Aerodynamic resolution angle, deg
ϕ_v	Spacecraft roll angle about the velocity vector, deg

DESCRIPTION OF SIMULATION

General

The computers used for this simulation were three AD80 analog computers and two DDP24 digital computers. The three analog computers were used to simulate in real time the vehicle dynamics during the entry phase of a lunar return trajectory. The analog outputs, equation solutions, were then fed via A-D converters to the DDP24 digital control computer and to the DDP24 digital aerodynamic computer. The aerodynamic computer took the analog information and calculated the required angular velocity for the centrifuge arm and gondola attitude position. This calculated data was then transmitted via the DDP24 control computer to the centrifuge servo control electronics which drove the centrifuge arm motor and gondola gimbal to properly simulate the acceleration forces acting on the command module. Also, the vehicle attitude signals (from the analog) were fed to the cockpit instruments via the DDP24 control computer. To close the loop, the pilot, using the attitude information and EMS (entry monitor system) information in addition to other information, sent commanded roll signals via the RHC (rotational hand controller) to the analog computer. Figure 1 is a flow diagram of the total system.

All computers, analog and digital, were in a first floor laboratory and the centrifuge and centrifuge electronics in a separate room in the Flight Acceleration Facility, Building 29. The two DDP24 digital computers were programmed and operated by System Test Branch personnel, Crew Systems Division. Besides controlling the centrifuge and cockpit instrumentation, the DDP24 computer had overall control of the total simulation mode status, that is, the analog modes (initial condition, hold, and operate) were controlled by signals from the DDP24 computer. This will be discussed in more detail in "special circuits." For more detail on the operation of the centrifuge and digital computers, see reference 1.

Description of Vehicle

Vehicle mass properties.- The command module mass, inertias, and center of gravity were all held constant. The vehicle mass characteristics were as follows:

Mass	= 402.6 slugs
I_x	= 6250.1 slug-ft ²
I_y	= 5851.2 slug-ft ²
I_z	= 5851.2 slug-ft ²
I_{xy}, I_{yz}, I_{zx}	= 0.0

The coordinates of the vehicle center of gravity expressed in terms of the standard Apollo coordinate system were $X_{cg} = 1041.6$ inches, $Y_{cg} = 0.0$ inches, and $Z_{cg} = 5.57$ inches. This center of gravity gave the vehicle a lift-to-drag ratio of .28 which was nominal for the Apollo 101 command module.

Vehicle RCS thrust characteristics.- During entry from .05 g altitude, the only control thrust available is from the CM RCS jets. For this simulation the rotational moments resulting from CM RCS jets were as follows:

$$\begin{array}{ll} +L_j = 473 \text{ ft-lbs} & -L_j = -452 \text{ ft-lbs} \\ +M_j = 513 \text{ ft-lbs} & -M_j = -340 \text{ ft-lbs} \\ +N_j = 478 \text{ ft-lbs} & -N_j = -480 \text{ ft-lbs} \end{array}$$

Rotational moments due to jet interaction were not considered.

Vehicle control system.- The command module reaction control system used to command the rotational moments consisted only of rate-command control mode with a rate deadband of +2 degrees/sec and a hysteresis of .2 deg/sec. Inputs into the control system were the pilot's commanded rotational rates via the rotational hand controller. The commanded rates were proportional to RHC deflection with a maximum command of 20 deg/sec. A block diagram of the control system is shown in figure 2.

Vehicle aerodynamic characteristics.- The command module which was simulated to have the aforementioned mass properties and an LOD (lift-to-drag ratio) of .280 was aerodynamically stable for earth entries at a trim angle of attack of 18.7 degrees. Angle of attack (η) is defined as the acute angle between the total velocity vector and the (-X) body axis. The equation defining angle of attack is

$$\eta = \arccos \left(\frac{-u}{V_T} \right) \text{ where: } V_T = \text{total velocity}$$

$$u = \text{projection of } V_T \text{ on X body axis}$$

Figure 3 is a diagram showing the angle of attack, η .

The axial and normal force coefficient slopes and pitching moment coefficient slope were considered linear and a function of cosine η and not as a function of Mach number. The equations used to define the aerodynamic coefficients are the following:

$$\begin{array}{l} C_A = C_{A_\eta} \cos \eta + K_2 \\ C_N = C_{N_\eta} \cos \eta + K_3 \\ C_m = C_{m_\eta} \cos \eta + K_4 \end{array}$$

where: Ordinate value C_A vs. $\cos \eta$ curve, $K_2 = 1.05$
 Ordinate value C_N vs. $\cos \eta$ curve, $K_3 = .7724$
 Ordinate value C_m vs. $\cos \eta$ curve, $K_4 = .3429$
 Axial force coefficient slope, $C_{A\eta} = -2.548$
 Normal force coefficient slope, $C_{n\eta} = -.7425$
 Pitching force coefficient slope $C_{m\eta} = -.31$

Equations of Motion

The EMS simulation equations were written only for the purpose of lunar return entry training for altitudes from 300,000 to 100,000 feet and therefore could be simplified to allow them to be programed on the three AD-80 analog computers which were available for the job. Although the two DDP24 digital computers were in use at the Flight Acceleration Facility, they were committed to control and monitoring functions and could not be used in the simulation of the entry vehicle. Even though some rather severe simplifications were made to the equations to fit them to the available computers, events proved that the equations were more than adequate for the objectives of the program.

Coordinate Systems.- Two coordinate systems were used in the reentry equations. The (1) inertial coordinate system, and (2) CSM or body coordinate system are defined in the following two paragraphs and are diagramed in figures 4 and 3 respectively.

The inertial coordinate system is an orthogonal axes system whose origin is coincident with the surface of the earth. The inertial X_I axis is parallel to the earth's surface and is positive pointing west. The Y_I axis is perpendicular to the X_I axis, parallel to the earth's surface, and is positive pointing north. The Z_I axis is positive pointing toward the earth's center and completes the right-handed triad.

The body coordinate system is an orthogonal system which is fixed to the vehicle and whose origin is on the command module longitudinal axis. The X_b axis is coincident with the vehicle longitudinal axis and is positive pointing through the apex of the command module. The Y_b axis is perpendicular to the X axis and is positive pointing through the pilot's right arm. The Z_b axis is positive pointing through the vehicle center of gravity and completes the right-handed triad.

Mathematical Model.- The math model (reference 2) used for this simulation was developed by Control Requirements Branch, Guidance and Control Division. The equations which are presented in block diagram form in figure 5 are written in six degrees of freedom and were simplified because of (1) the limitation of analog equipment, (2) limited time available to mechanize the equations, and (3) limited objectives (simulation was to be used only for astronaut crew training). However, the equations were sufficiently detailed to correctly calculate the vehicle dynamics and accelerations necessary to simulate lunar entries from .05 g (300,000 ft altitude) to 100,000 ft altitude. In addition to the normal spacecraft equations of motion, the EMS range-to-go equations (reference 3) were mechanized and solved on the computers.

The principal simplifications and assumptions made in writing the equations were as follows:

- a. The earth model is a non-rotating cylinder with a constant gravitational force.
- b. Spacecraft position calculations are omitted except for altitude.
- c. Cross-coupling inertia and products of inertia terms are omitted.
- d. RCS jet interaction terms have been omitted.
- e. Center of gravity offset in the Y_B axis has been neglected.
- f. Aerodynamics are functions of total angle of attack only and are considered linear functions of the cosine of the angle of attack.
- g. Mass and inertia characteristics are constant.

Special mention should be made of the first assumption. A centrifugal force term is subtracted from the gravitational force and this difference is multiplied by a gravity gain factor (K_g in the equation). This factor was adjusted experimentally so that the duration of the runs and the maximum acceleration were approximately the same as those obtained in more sophisticated simulations.

Inputs to the equations of motion were the commanded rotational rates from the pilot's three axes RHC (rotational hand controller in the cockpit).

The analog outputs (solutions of the equations) were recorded on two eight-channel strip chart recorders. In addition, three of these, the spacecraft attitude, EMS roll stability attitude, and the vehicle applied accelerations, were sent to the Honeywell digital computer.

Analog Mechanization

The equations of motion mechanized on the analog computers are shown in a detailed block diagram in figure 5. A majority of the mechanization was of standard configuration and no attempt will be made to explain the entire program. However, some explanation will be given on three of the circuits:

a. Generation of $\sin \phi_B$, $\cos \phi_B$, V_T , and $\cos \eta$.- The technique used to compute the trigonometric functions of the aerodynamic angles and the total velocity was based on a paper by Robert M. Turner (reference 4). It is an implicit or bootstrap method which solves an equation of the type $R = X \cos \theta + Y \sin \theta$ where $R = \sqrt{X^2 + Y^2}$ and $\theta = \tan^{-1} Y/X$ rather than the more straightforward computations $R = \sqrt{X^2 + Y^2}$, $\sin \theta = \frac{Y}{\sqrt{X^2 + Y^2}}$ and $\cos \theta = \frac{X}{\sqrt{X^2 + Y^2}}$. The implicit technique eliminates the square root circuits and places the inverse trigonometric functions inside a closed loop. Experience has shown that this technique is more accurate and more stable than the more conventional technique when the total angle of attack approaches zero. When this happens, both X and Y approach zero and the conventional circuits run into trouble by attempting to divide one small quantity by another small quantity. Circuit diagrams are shown in figure 6.

b. Generation of dynamic pressure, \bar{q} .- The atmospheric density, ρ , varies by a factor of nearly 10^4 for the altitude range encountered during an entry. If ρ were generated directly then at an altitude above, say 200,000 feet, the signal-to-noise ratio would be so low that accurate generation of dynamic pressure would be impossible. This difficulty was avoided by generating $\rho^{\frac{1}{4}}$, squaring it, multiplying this variable by velocity, and finally squaring $\rho^{\frac{1}{2}} V$ to obtain dynamic pressure. To use the full range of the function generator, the function $(2\rho^{\frac{1}{4}} - \rho_{\max}^{\frac{1}{4}})$ versus $(h - 200,000)$ was programmed. Details of mechanization are given in figure 7.

c. Mode control of the analog integrators.- For checkout and operational purposes, the three analog computers were slaved together with one computer acting as the master. Under these conditions the operational modes, initial conditions (IC), hold (H) and operate (OP), of the slave computers are synchronized to those of the master computer. For ease and convenience of checkout and operation, the mode control signals were generated at two different sources, the master analog computer and the DDP24 digital control computer with the control signals being gated to the analog computers by a switch on the master analog console logic board. The operational philosophy employed was to use the master analog control signals during open loop testing (unit checkout) and to use the digital control

signals during the analog-digital-centrifuge closed loop runs. The logic circuitry required for the optional control of the analog integrators is shown in figure 8.

Run Termination.- The aforementioned mode control signals were also used to terminate the data runs, that is, put the integrators into hold mode. There were two, normal and abnormal, types of terminate criteria to stop a close loop run. The normal run termination took place when the vehicle altitude reached 100,000 feet. Abnormal termination occurred when an analog amplifier overload lasted longer than one second, or a hardware failure other than the analog computers occurred, such as digital hardware failure, centrifuge overspeed, major power failure, or if the medical officer or pilot determined the run ought to be stopped.

The altitude and analog amplifier overload terminate signals were generated on the analog and sent to the digital control computer where they were combined with the other terminate signals, and the digital control computer in turn sent a hold signal back to the analog integrators. At the same time, the digital control computer also sent control signals to the centrifuge to decrement the centrifuge arm speed to a level of 1G at a rate of $1/16$ G per second. The circuits used to generate these termination signals are shown in figure 8.

RESULTS AND DISCUSSION

The EMS simulation was used to train the Apollo 8 prime crew (Borman, Lovell, Anders) and backup crew (Armstrong, Aldrin, Haise) for two days - 1 day in shirt sleeves and 1 day in vented suits, the Apollo 10 command pilot (John Young) for one day; and one additional day using two pilots (R. Lindsay and M. Lake) from Flight Crew Support Division was used to determine if entries could be made using a limited amount of visual cues (that is, no EMS instrumentation). It was demonstrated that safe lunar return entries could be made using only a G meter and a roll attitude indicator as visual cues.

The initial conditions for the various entry profiles that were flown to take data are given in table 1 with all runs beginning at approximately 300,000 feet with the lift vector up. During each run the command module stayed in free flight from 300,000 feet to .05 g's ($\approx 290,000$ ft) at which time the pilot took over the controls and flew to a precalculated EMS target at 100,000 feet altitude. Two techniques (1) EMS ranging and (2) constant g profiles were used to fly to the precalculated target. The success of the run was determined by how close to zero the RTG counter read at the end of the run, i.e., when altitude $\approx 100,000$ feet. An example of the analog recorded results from a constant 3 g profile run is shown in figure 9.

During the actual data runs, the simulation flew with no analog or digital computer failures. Troubles that did occur during the data runs occurred in the cockpit instrumentation, (1) EMS RTG counter, (2) the G-meter, and (3) roll stability indicator (RSI) meter. These instrument troubles were minor and did not hamper the operation of the simulation in taking data. The troubles were intermittent and were of the type where the instrument needle or indicator did not follow the analog-digital signal that was sent to them.

Digital Verification of the EMS Math Model

To validate the EMS equations of motion, a digital simulation using a fourth order Runge-Kutta integration routine with a .15 sec. step size was run and the results compared with a supercircular entry run from the CSM Guidance and Control Verification Simulation (CSM G&CVS). The EMS equations of motion were considered verified when the plots of altitude, total velocity, and dynamic pressure versus time followed the same general pattern of those from the CSM G&CVS.

Following this, additional digital runs were made to obtain the proper gravity coefficient gain factor, K_1 (required in the EMS equations to compensate for the non-rotating earth). The gain factor was determined by the agreement of the EMS plots of altitude, dynamic pressure, and velocity versus time with similar plots from the CSM G&CVS simulation. A $K_1 = 1.06$ was required and the compared plots are shown in figure 10.

A further check on the equations of motion was performed when the digital program was used to generate range-to-go (RTG) numbers for a constant G range-to-go chart. To obtain the RTG numbers, additional guidance equations (reference 3) were added to the digital program to make the vehicle automatically fly constant G entry profiles. These additional equations shown in figure 11 were used to obtain range-to-go numbers for constant 2, 3, 4, and 5 G's for the four cases used to take close loop data. These RTG numbers were charted for the various constant G runs and then used to initialize the EMS RTG counter prior to each data run. The EMS range-to-go results compared with MPAD's constant G entry RTG numbers within 0-100 n.m. for 800-1600 n.m. runs. Comparison of the two sets of RTG numbers were tabulated and are shown in table 2.

Dynamic Check of the Analog Mechanization

Three types of runs using lunar return entry initial conditions were used to dynamically verify the analog mechanization of the EMS equations. The success criteria for the analog mechanization was to compare the analog solutions of the three runs with digital solutions of the identical runs. The three types of runs were:

1. No aerodynamics (zero dynamic pressure).

2. Constant bank angle ($\phi = -90^\circ$) with aerodynamics.
3. Continuous $20^\circ/\text{s}$ rolling entry with aerodynamics.

The comparison of the digital and analog dynamic solutions of these runs are shown in figures 12, 13, and 14.

Initially during the checkout period a considerable amount of trouble was encountered in obtaining satisfactory analog solutions for these runs, that is, to match the digital solutions. The trouble was discovered to be an offset in $\dot{\theta}$, rate of change of the Euler pitch angle which resulted in a drift in the vertical velocity. The offset was constant for a particular day but would change from day to day. Initially (when it was first discovered), the $\dot{\theta}$ offset was 0.75 milliradian/sec but this was due to a bad multiplier in the circuit forming $\dot{\theta}$. This was replaced and the offset dropped to 0.10 - 0.30 milliradians/sec depending on the day. To compensate for this offset, a bias voltage was added to the $\dot{\theta}$ circuitry which temporarily eliminated the drift. However, long term changes in the multiplier offset, which were within normal drift tolerances, required that a careful and almost continued check be made on the sensitive circuit. This problem is discussed in more detail in reference 5 and in the appendix of this paper.

CONCLUDING REMARKS

A simplified set of equations was used in a closed loop entry simulation to train the Apollo 8 prime and backup crews. The equations of motion were solved on analog computers, the outputs of which were used as drive signals for the Flight Acceleration Facility centrifuge. The digital solutions of the simplified equations and the actual piloted data runs verified the equations to be adequate for the purpose of training pilots for lunar entries. The digital verification results of the EMS equations agreed with results obtained from the CSM G&CVS simulation and from an MPAD digital entry simulation. In addition to training the Apollo 8 crews, the simulation was used to demonstrate that safe entries could be made from lunar return velocities using only a meter for an indication of roll angle and an accelerometer as instruments.

During the actual data runs the simulation operated with no failures or major problems with the analog or digital computers. However, during the checkout phase a sensitivity problem was encountered in solving the equations of motion. This resulted in a drift in vertical velocity which was eliminated only by a careful and almost continued check on the sensitive circuit. The equations have been modified in an attempt to reduce or eliminate the sensitivity and it is recommended that the modified equations be programmed to determine if the sensitivity has, indeed, been eliminated.

REFERENCES

1. Harron, Ronald S. "Test Procedures, Closed Loop Centrifuge Training Program Using the Entry Monitoring System." October 8, 1968.
2. Gardiner, Robert A. "Math model for EMS closed loop entries using the flight acceleration facility." Tech. memo. No. EG27-265-68-1028, September 20, 1968.
3. Gilbert, David W. "Generation of Entry Monitor System initial conditions for the centrifuge math model." Tech. memo. No. EG27-68-285, October 8, 1968.
4. Turner, Robert M. "On the Reduction of Error in Certain Analog Computer Calculations by the Use of Constraint Equations," Proceedings of the Western Joint Computer Conference, May 3-5, 1960.
5. Russell, W. R. "Simplified equations of motion for entry simulations." Tech. memo. No. EG24-68-215, October 24, 1968.

APPENDIX

Modifications to Equations of Motion for Entry Simulation

The equations of motion used in the entry simulations seemed to be unusually sensitive to small errors in the computation of $\dot{\theta}$, the derivative of the pitch Euler angle. The reason for this can be seen by the following analysis.

Starting with the equations as given in figure 5 and assuming that the yaw angle, yaw rate, lateral velocity, rolling velocity, and roll angle and dynamic pressure are all zero, the equations of motion can be written as:

$$\dot{u} = -g_e \sin \theta$$

$$\dot{w} = g_e \cos \theta$$

$$\dot{\theta} = \epsilon$$

$$\dot{h} = u \sin \theta - w \cos \theta$$

$$g_e = g - V_T^2/R$$

where u and w are the x- and y-body components of the velocity, θ is the pitch angle, h is the altitude, ϵ is an assumed error in the computation of $\dot{\theta}$, V_T is the total velocity, g the gravitational acceleration and R the radius of the earth.

Taking the derivative of \dot{h} with respect to time,

$$\begin{aligned} \ddot{h} &= \dot{u} \sin \theta - \dot{w} \cos \theta \\ &\quad + \dot{\theta}(u \cos \theta + w \sin \theta) \end{aligned}$$

which simplifies to

$$\ddot{h} = -g_e + \dot{\theta}(u \cos \theta + w \sin \theta).$$

But $u \cos \theta + w \sin \theta$ is approximately equal to the total velocity, V_T and thus

$$\ddot{h} = -g_e + \epsilon V_T.$$

In the entry simulation, the static offset in $\dot{\theta}$ was about 0.75 milliradians/second and the velocity was about 36,000 feet/second. The resulting error in vertical acceleration was 27 ft/sec², the same order of magnitude as the gravitational acceleration.

If the equations are written so that the translational acceleration-to-velocity integrations are done in a non-rotating coordinate system, this problem would be eliminated. A suitable set of equations follows without derivation. The assumptions inherent in these modified equations are basically the same as for the original equations. In addition, simplified equations were used to compute the angles of attack and sideslip and it was assumed that the lateral acceleration was negligible. This was done to reduce the number of coordinate transformations. No changes were made in the equations for the Entry Monitor System or the control system.

I. Aerodynamic-force equations

$$A_{x_b} = -C_A \bar{q} S/m$$

$$A_{y_b} = 0$$

$$A_{z_b} = -C_N \bar{q} S/m$$

II. Angular accelerations

$$\dot{p} = C_Y \frac{Z_{cg}}{D} \frac{\bar{q}SD}{I_x} + \frac{L_j}{I_x}$$

$$\dot{q} = \left(C_m + \frac{Z_{cg}}{D} C_N \right) \frac{\bar{q}SD}{I_y} + \frac{M_j}{I_y}$$

$$\dot{r} = C_n \bar{q}SD/I_z + N_j/I_z$$

III. Euler rates - pitch, yaw, roll sequence

$$\dot{\psi} = q \sin \phi + r \cos \phi$$

$$\dot{\theta} = (q \cos \phi - r \sin \phi) / \cos \psi$$

$$\dot{\phi} = p - \dot{\theta} \sin \psi$$

IV. Aerodynamic accelerations, inertial axes (assume $A_{y_b} = 0$)

$$A_{x_1} = A_{x_b} \cos \psi \cos \theta + A_{z_b} (\cos \phi \sin \theta + \sin \phi \sin \psi \cos \theta)$$

$$A_{y_1} = A_{x_b} \sin \psi - A_{z_b} \sin \phi \cos \psi$$

$$A_{z_1} = -A_{x_b} \sin \theta \cos \psi + A_{z_b} (\cos \phi \cos \theta - \sin \phi \sin \psi \sin \theta)$$

V. Total inertial accelerations

$$\dot{V}_x = A_{x_1}$$

$$\dot{V}_y = A_{y_1}$$

$$\begin{aligned} -\dot{V}_{z_1} &= -A_{z_1} + \left(\frac{V_H^2}{R} - g \right) K_1 \\ &\approx -A_{z_1} + \left(\frac{V_T^2}{R} - g \right) K_1 \end{aligned}$$

VI. Miscellaneous velocities and angles

$$V_H = (V_x^2 + V_y^2)^{\frac{1}{2}}$$

$$V_T = (V_H^2 + V_z^2)^{\frac{1}{2}}$$

$$\dot{h} = -V_z$$

$$\begin{aligned} \gamma &= \text{flight path angle} \\ &= \tan^{-1} \frac{\dot{h}}{V_H} \end{aligned}$$

$$\approx \dot{h}/V_H$$

$$\begin{aligned}\psi_h &= \text{heading angle} \\ &= \tan^{-1}(-v_y/-v_x) \\ &= \sin^{-1}(-v_y/v_H)\end{aligned}$$

$$\begin{aligned}\alpha &= \text{angle of attack} \\ &= \tan^{-1}(w/|u|) \\ &\approx -[(\theta + \gamma)\cos\phi + (\psi - \psi_h)\sin\phi]\end{aligned}$$

$$\begin{aligned}\beta &= \text{angle of sideslip} \\ &= \sin^{-1}(v/v_T) \\ &\approx -[(\theta + \gamma)\sin\phi - (\psi - \psi_h)\cos\phi]\end{aligned}$$

$$\begin{bmatrix} u \\ v \\ w \end{bmatrix} = \begin{bmatrix} l_1 & l_2 & l_3 \\ m_1 & m_2 & m_3 \\ n_1 & n_2 & n_3 \end{bmatrix} \cdot \begin{bmatrix} v_x \\ v_y \\ v_z \end{bmatrix}$$

VII. Aerodynamic coefficients and dynamic pressure

$$\begin{aligned}C_A &= \text{axial force coefficient} \\ &= C_{A_0} + C_{A_1} \alpha^2\end{aligned}$$

$$\begin{aligned}C_N &= \text{normal force coefficient} \\ &= C_{N_0} + C_{N_1} \alpha\end{aligned}$$

$$\begin{aligned}C_Y &= \text{lateral force coefficient} \\ &= C_{Y\beta} \beta\end{aligned}$$

$$\begin{aligned}C_m &= \text{pitching moment coefficient} \\ &= C_{m_0} + C_{m_1} \alpha\end{aligned}$$

IX. Constants

$$m, I_x, I_y, I_z, Z_{cg}, S, D, g, R$$

$$C_{A_0}, C_l, C_{N_0}, C_{N_\alpha}, C_{Y_\beta}, C_{m_0}, C_{m_\alpha}$$

$$C_{n_\beta}, L_j, M_j, N_j, \alpha_t$$

Function of altitude

$$\rho = \text{mass density of air}$$

The modified equations have been programed and checked out for the three AD80 analog computers used in the original simulations and a digital check simulation has been obtained. The results of these simulations have been compared with results obtained from more elaborate simulations such as the Command Module G&C Verification Simulation and generally good agreement has been obtained. Figure 15 is a comparison of results for a rolling entry obtained from the simplified analog simulation and results obtained from the Command Module G&C Verification Simulation study. As an inspection of the figure shows, there is good agreement between the two simulations. The differences in the dynamic pressure probably arise from differences in the roll rate or other minor differences in the control system. Although not shown on the figure, the short period dynamic characteristics are also in good agreement. The same control system was used in the modified equations as in the original equation and hence the control characteristics which were reported to be good in the original simulation should be equally good with the revised equations.

The modification to the equations have removed the undue sensitivity encountered in the original equations and no new undesirable characteristics have been experienced. These facts coupled with the good agreement with the hybrid entry simulation make it advantageous to use the modified equations in future entry simulations where there are severe restrictions on the amount of computing equipment.

C_n = yawing moment coefficient

$$= C_{n\beta} \beta$$

\bar{q} = dynamic pressure

$$= \frac{1}{2} \rho V_T^2$$

VIII. Direction cosines

$$l_1 = \cos \theta \cos \psi$$

$$l_2 = \sin \psi$$

$$l_3 = -\sin \theta \cos \psi$$

$$m_1 = \sin \theta \sin \phi - \cos \theta \sin \psi \cos \phi$$

$$m_2 = \cos \psi \cos \phi$$

$$m_3 = \cos \theta \sin \phi + \sin \theta \sin \psi \cos \phi$$

$$n_1 = \sin \theta \cos \phi + \cos \theta \sin \psi \sin \phi$$

$$n_2 = -\cos \psi \sin \phi$$

$$n_3 = \cos \theta \cos \phi - \sin \theta \sin \psi \sin \phi$$

NOTE: Only six of the nine direction cosines are needed. The direction cosines m_1 , m_2 , and m_3 are not required.

FLIGHT PATH ANGLE AT H = 400000 FEET (DEG)	U (FT/SEC)	V (FT/ SEC)	W (FT/ SEC)	P (DEG/ SEC)	C (DEG/ SEC)	R (DEG/ SEC)	Θ (DEG)	Ψ (DEG)	Φ (DEG)	Φ_v (DEG)	H (FEET)
$\gamma = -5.75$	-34241.3	0	11591.	0	0	0	23.02	0	180	0	298887.
$\gamma = -6.00$	-34244.1	0	11591.	0	0	0	23.23	0	180	0	294695.
$\gamma = -6.40$	-34242.3	0	11591.	0	0	0	23.76	0	180	0	298420.
$\gamma = -7.10$	-34246.0	0	11591.	0	0	0	24.56	0	180	0	293480.

TABLE 1 INITIAL CONDITIONS FOR CLOSE LOOP DATA RUNS.

FLIGHT PATH ANGLE AT 400000 FEET (DEG)	CONSTANT G PROFILES (G'S)	RANGE TO GO FROM .05G'S, ≈290000 FEET ALTITUDE, TO 100000 FEET ALTITUDE (NAUTICAL MILES)		
		EMS	MPAD	ΔRTG
$\gamma = -5.75$	2	1643	1648	5
	3	1297	1312	15
	4	1067	1069	2
	5	909		
$\gamma = -6.00$	2	1523	1513	10
	3	1217	1199	18
	4	1013	1016	3
	5	878		
$\gamma = -6.4$	2	1391	1463	72
	3	1125	1173	48
	4	943	968	25
	5	829		
$\gamma = -7.1$	2	1136	1223	93
	3	941	1038	97
	4	807	860	53
	5	718		

TABLE 2. EMS DIGITAL RTG VALUES COMPARED WITH THOSE FROM AN MPAD (MISSION PLANNING AND ANALYSIS DIVISION) DIGITAL ENTRY SIMULATION FOR ENTRIES FROM .05G'S TO 100000 FEET ALTITUDE.

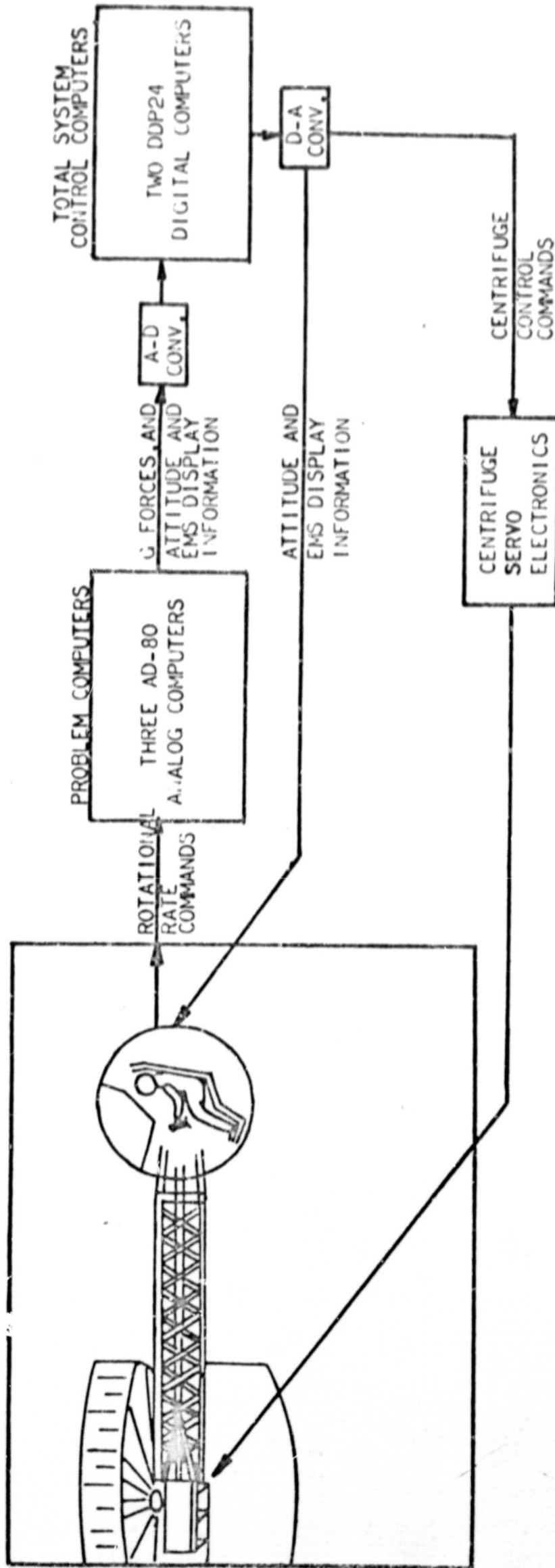


FIGURE 1 BLOCK DIAGRAM OF TOTAL SYSTEM

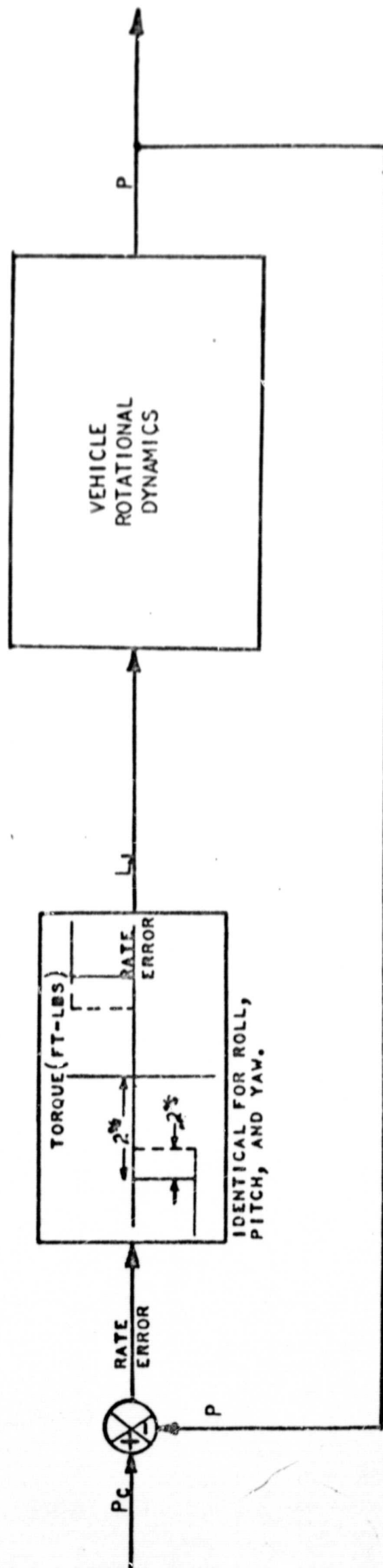


FIGURE 2 BLOCK DIAGRAM OF RCS RATE COMMAND CONTROL SYSTEM. ROLL CHANNEL SHOWN. PITCH AND YAW CHANNELS ARE SIMILAR.

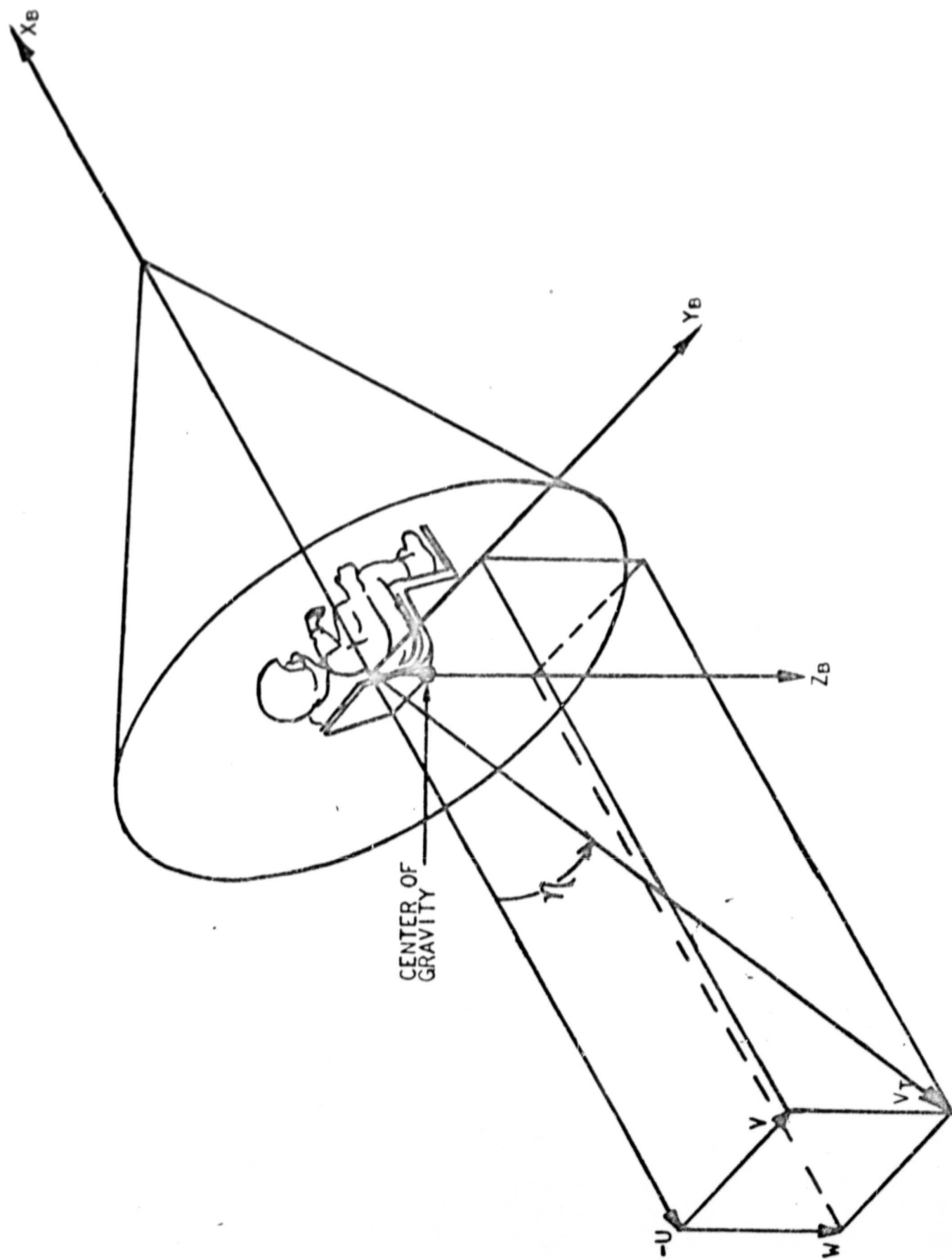


FIGURE 3 DIAGRAM SHOWING VEHICLE COORDINATE SYSTEM, VEHICLE CENTER OF GRAVITY, AND ANGLE OF ATTACK.

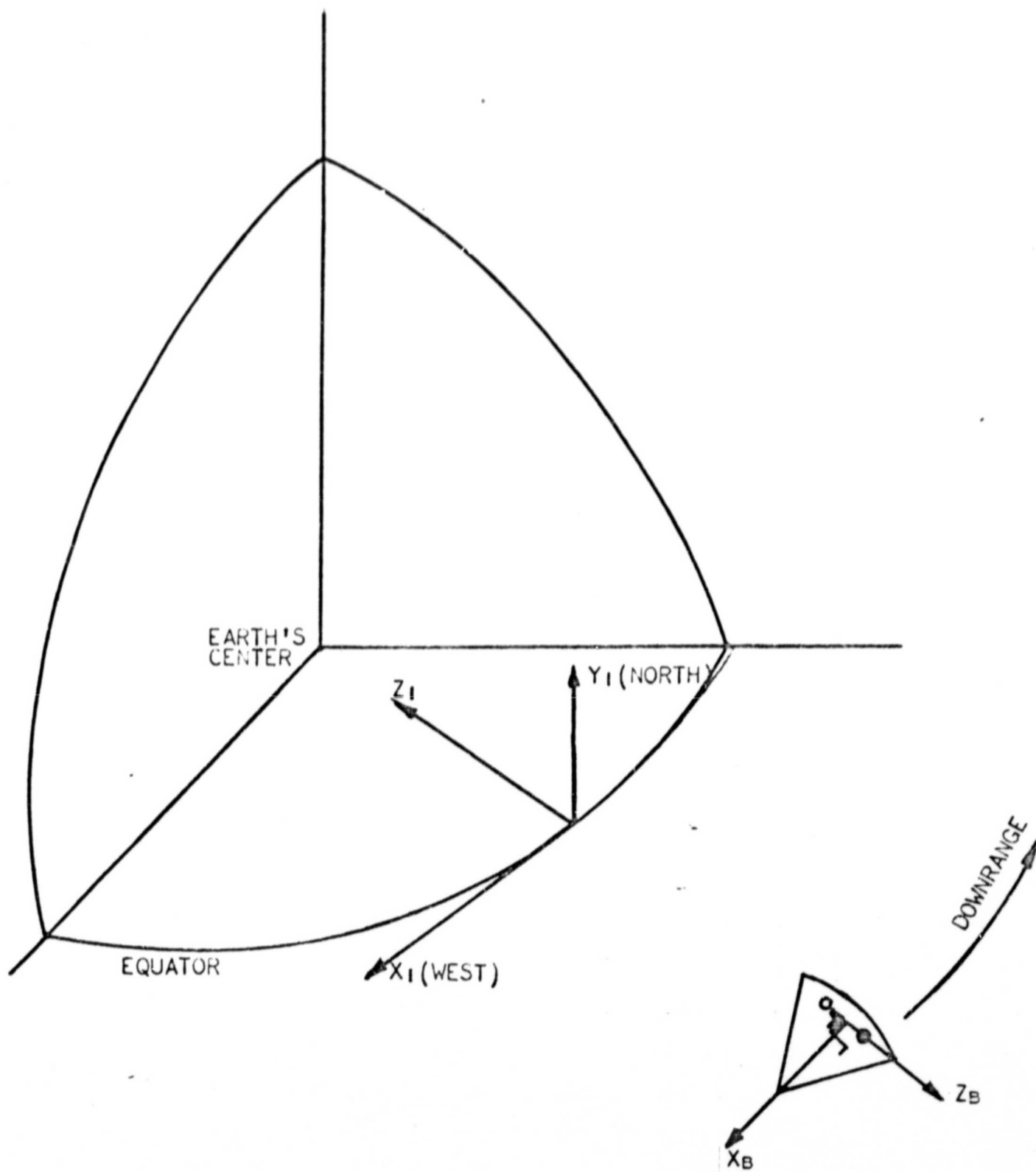


FIGURE 4 DIAGRAM SHOWING ORIENTATION OF INERTIAL COORDINATE SYSTEM

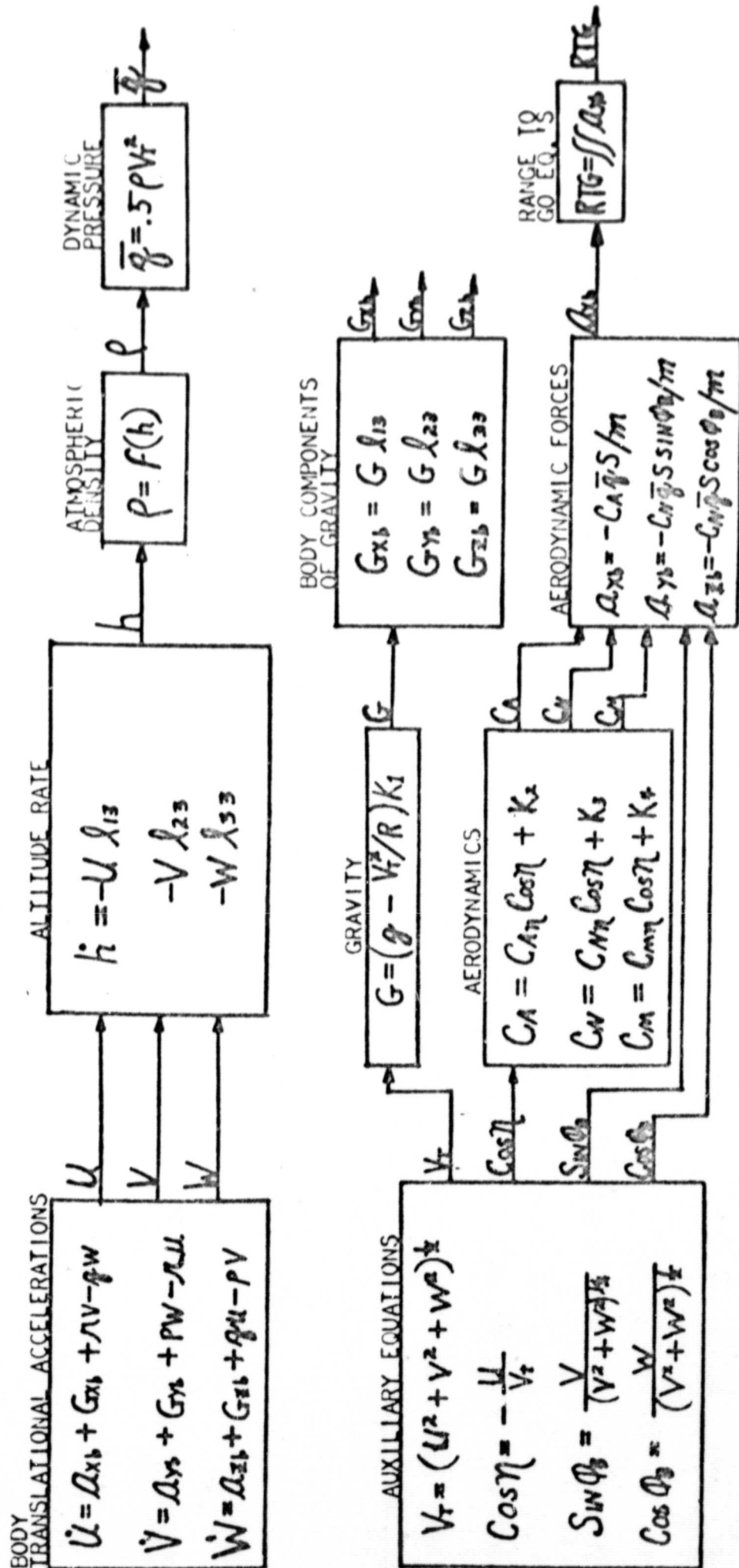
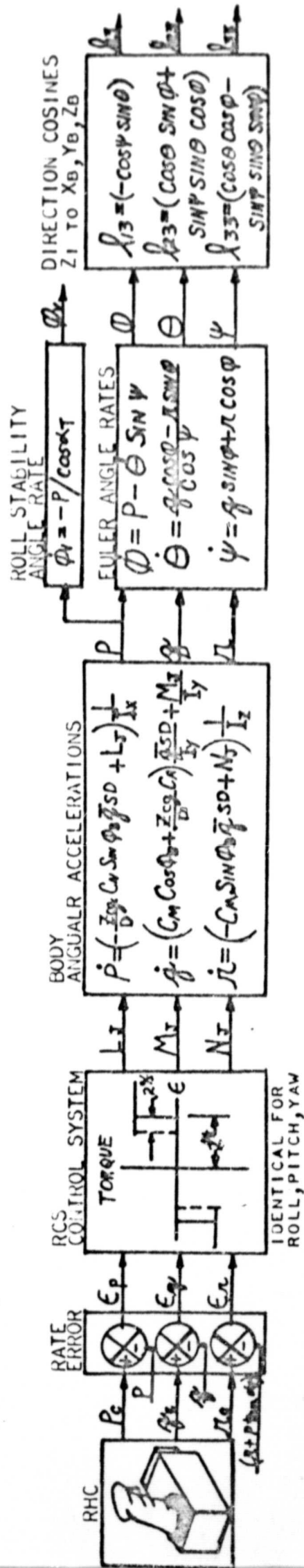


FIGURE 5 BLOCK DIAGRAM OF LPS MATH MODEL

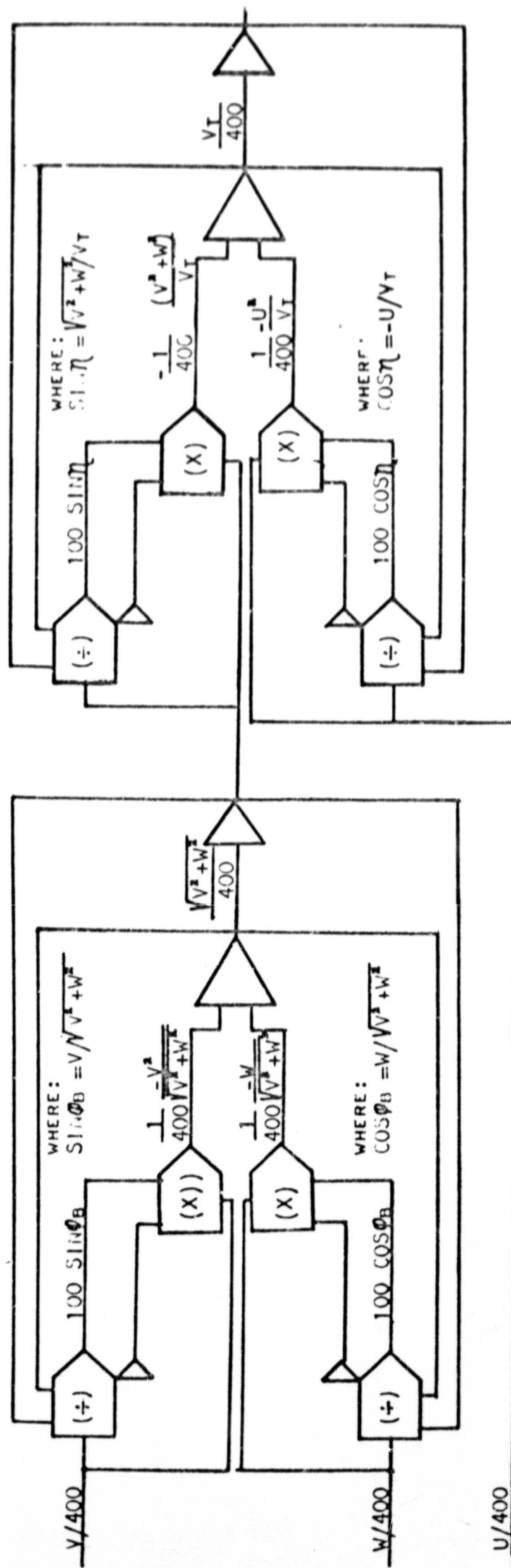
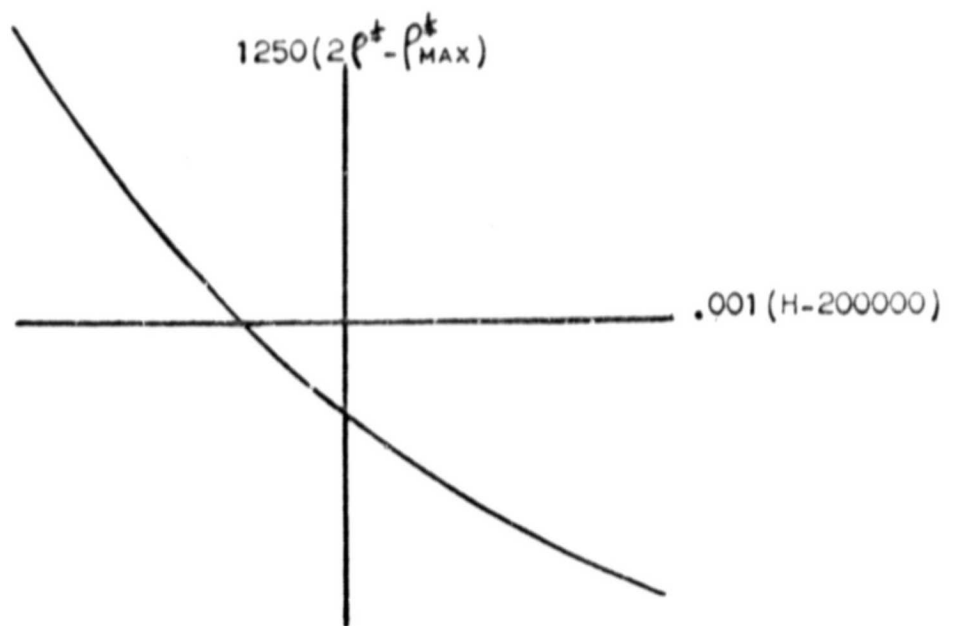


FIGURE 6 ANALOG CIRCUIT USED TO GENERATE $\sin(\phi_B)$, $\cos(\phi_B)$, $\sin(\eta)$, $\cos(\eta)$, V_T



PLOT OF DENSITY FUNCTION $[1250(2p^* - p_{MAX}^*)]$ SET UP ON 20 SEGMENT DFG

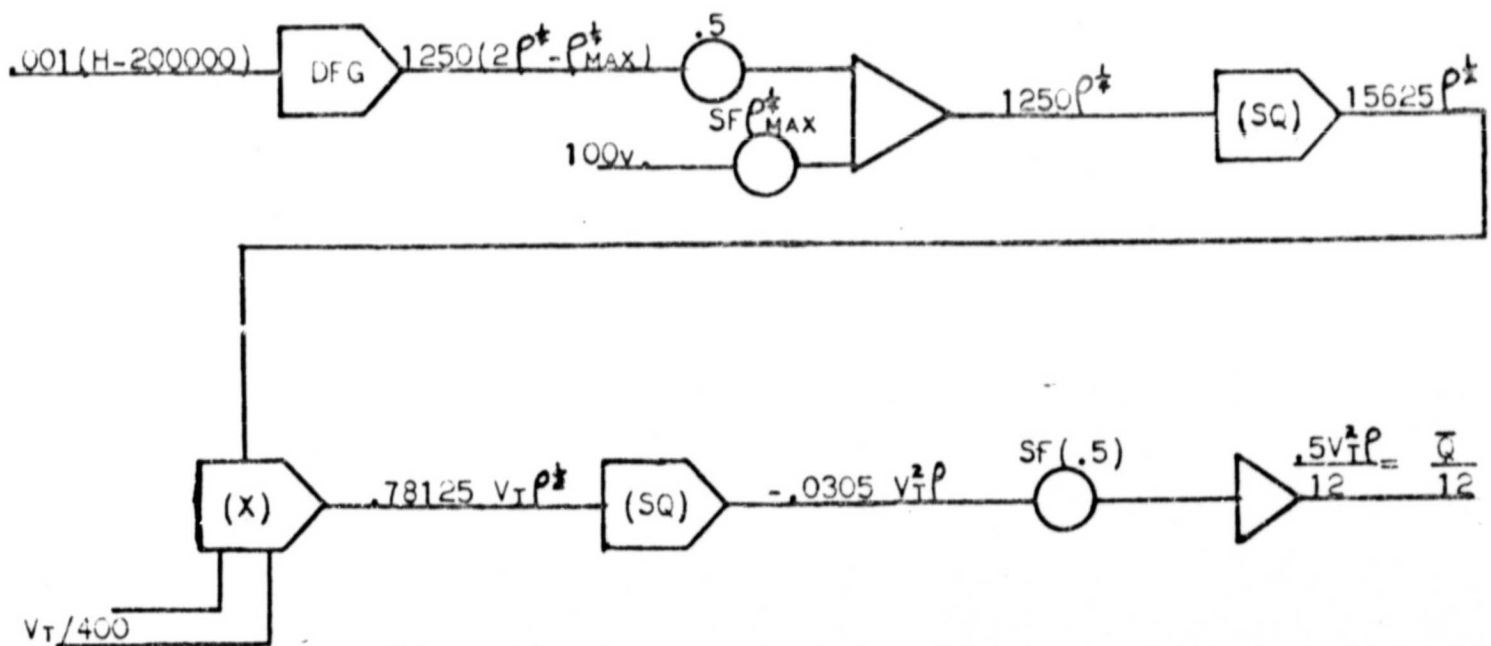
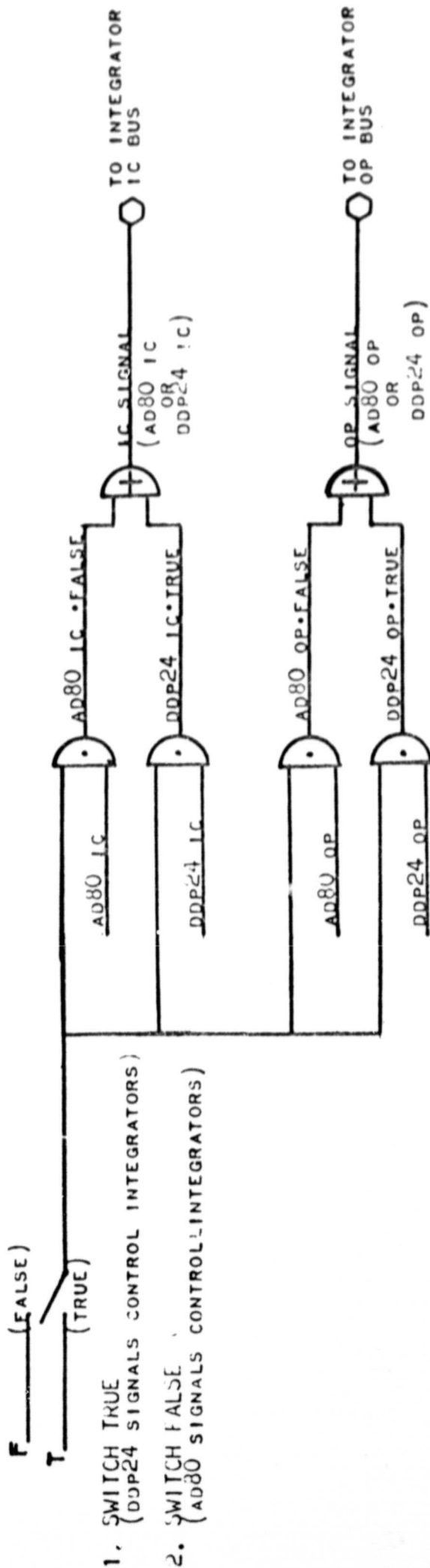


FIGURE 7 ANALOG CIRCUIT USED TO GENERATE DYNAMIC PRESSURE.



CIRCUIT USED FOR OPTIONAL (DIG/ANALOG) MODE CONTROL OF ANALOG INTEGRATORS

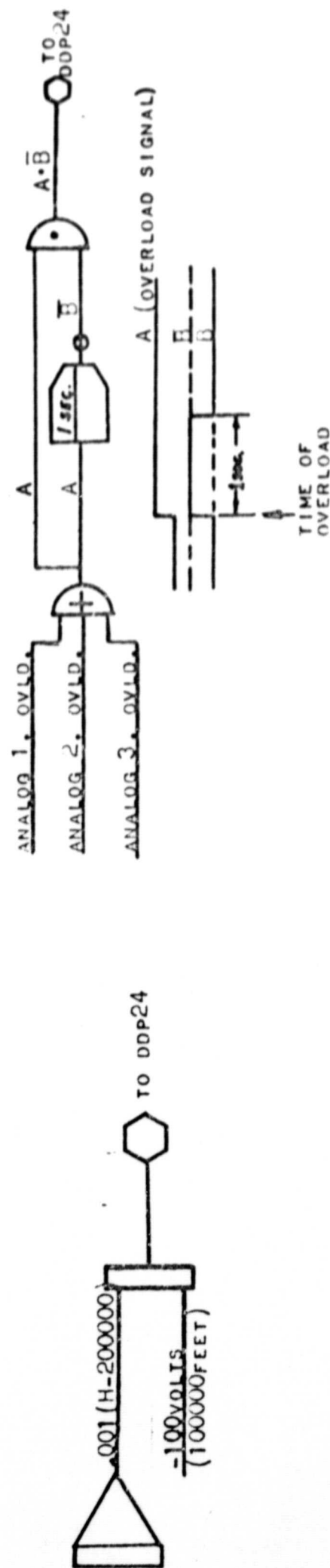


FIGURE 8 ANALOG MODE CONTROL CIRCUITRY

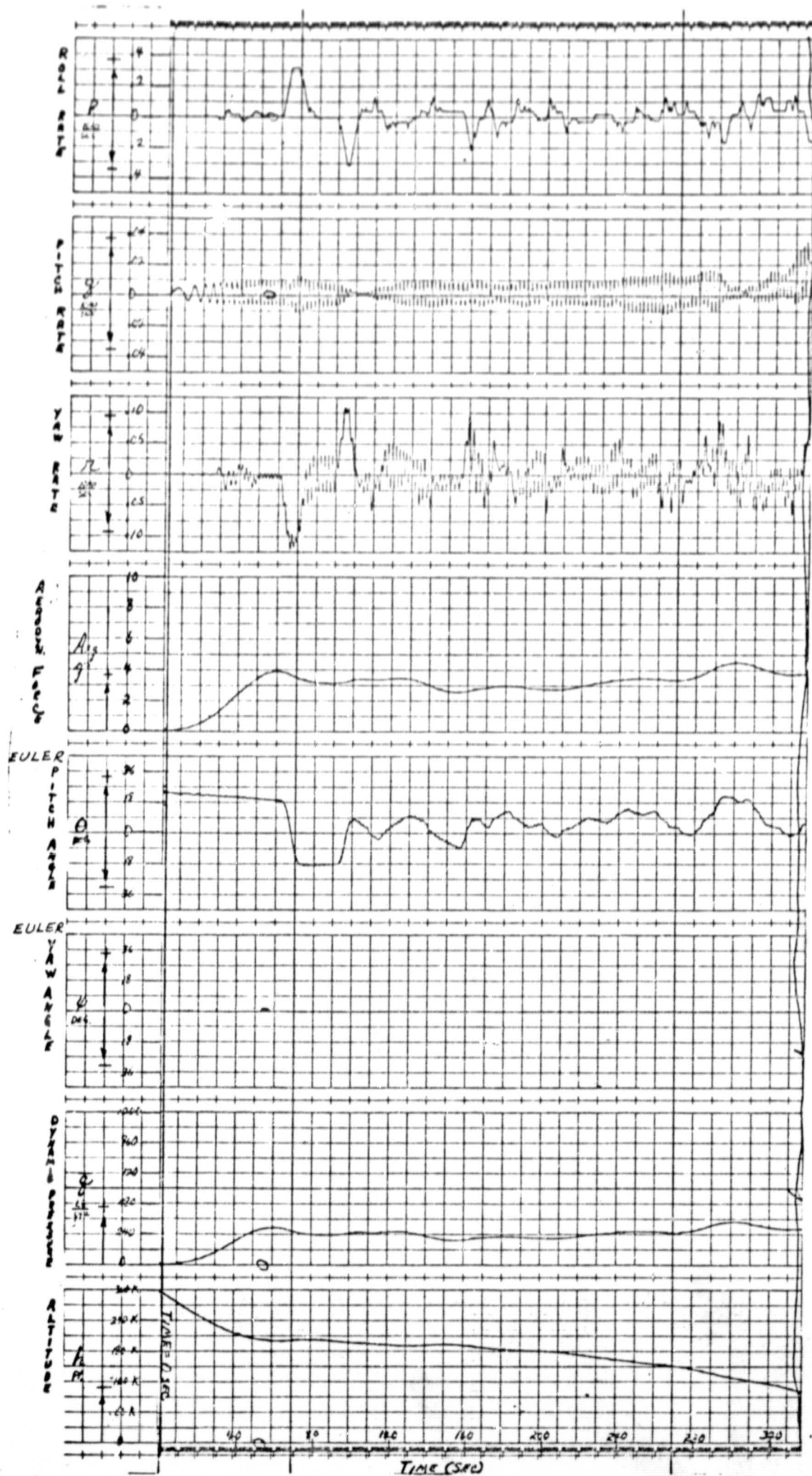


Figure 9 - Typical analog time history recordings from a piloted data run using case 2 initial conditions ($\gamma = 6.00^\circ$, table 1).

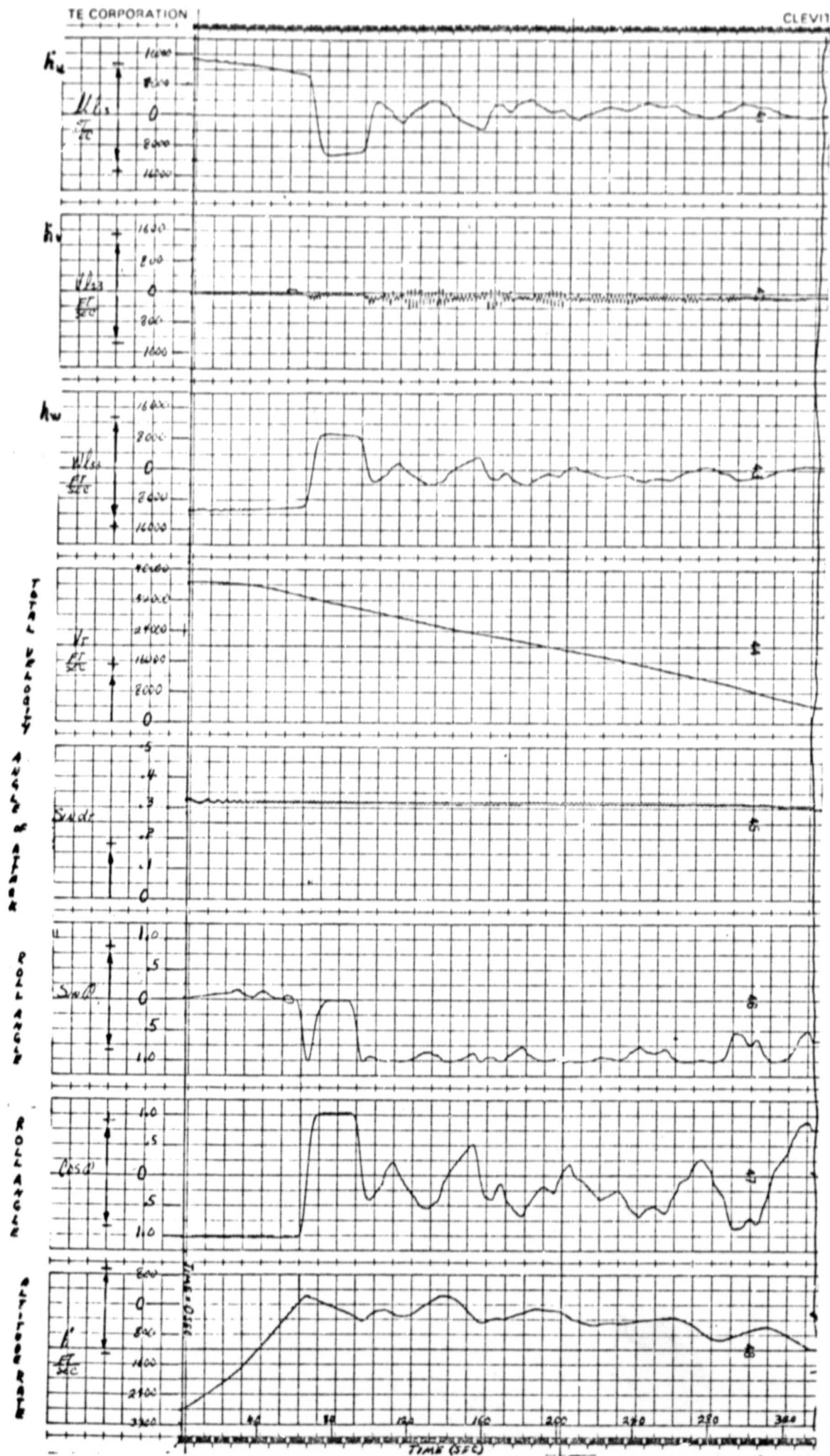


Figure 9 - continued

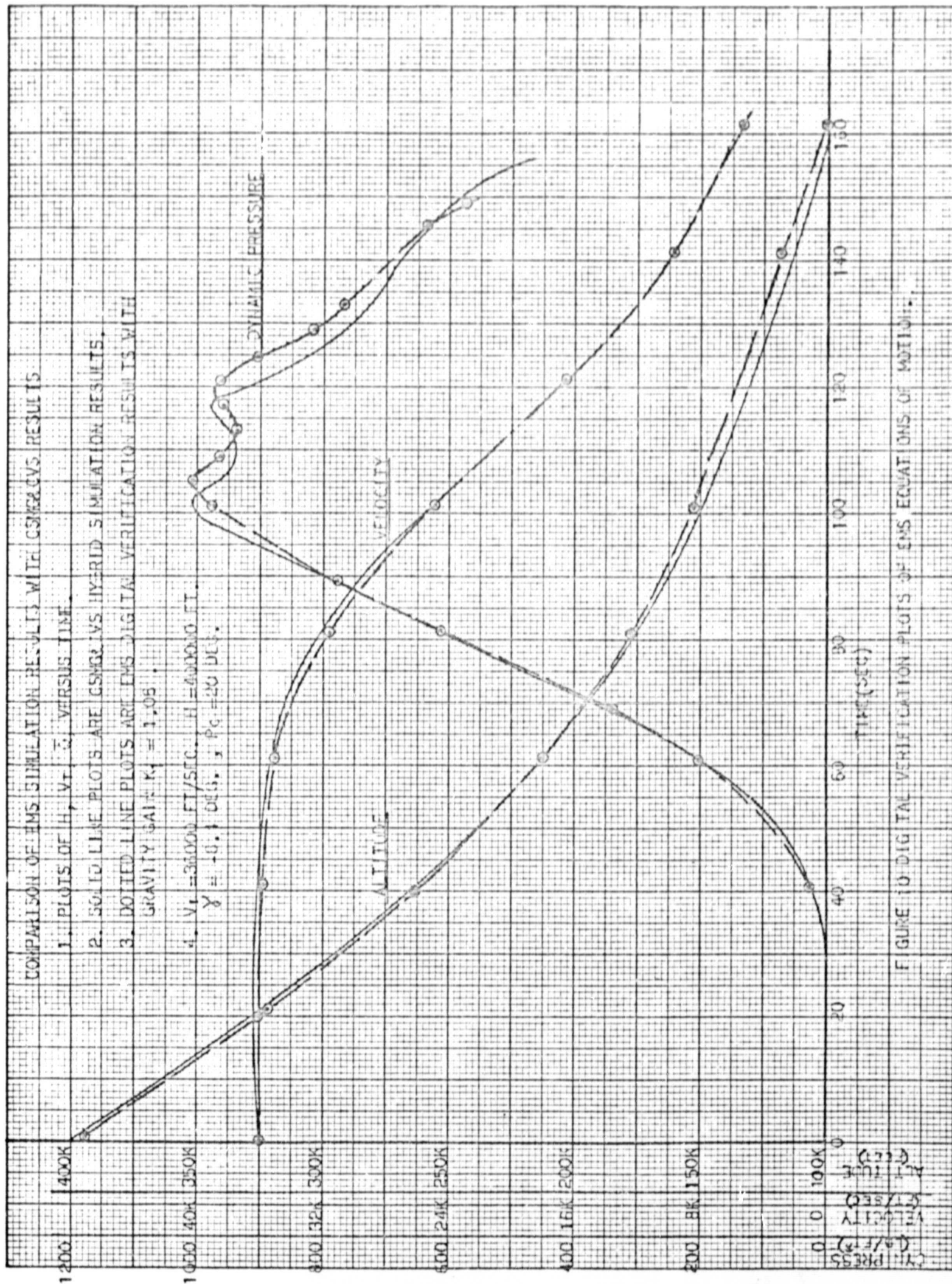
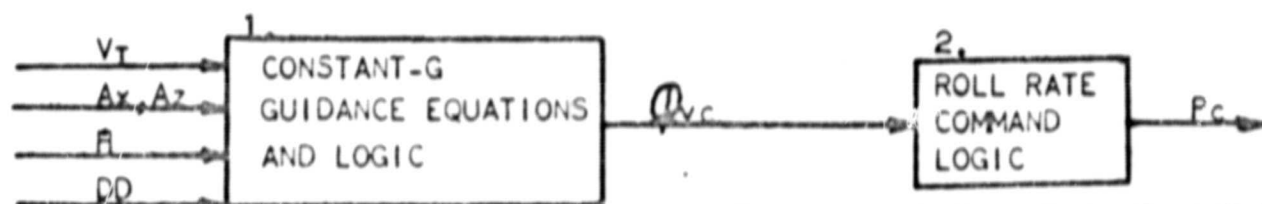


FIGURE 10 DIGITAL VERIFICATION PLOTS OF EINS EQUATIONS OF MOTION.

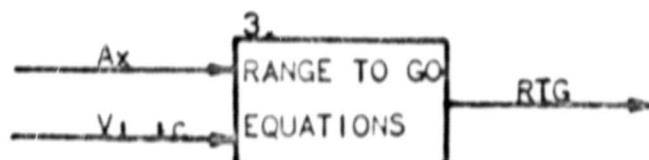
1. CONSTANT-G GUIDANCE EQUATIONS AND LOGIC

2. ROLL RATE COMMAND LOGIC

3. RANGE TO GO EQUATIONS



WHERE: V_T = TOTAL VEHICLE ACCELERATION
 A_x, A_z = APPLIED ACCELERATIONS
 \dot{H} = ALTITUDE RATE
 DD = DESIRED DRAG
 ϕ_{vc} = LIFT VECTOR COMMAND ATTITUDE
 P_c = ROLL RATE COMMAND
 $V_i(t) = V_{XB}$ AT .05G'S

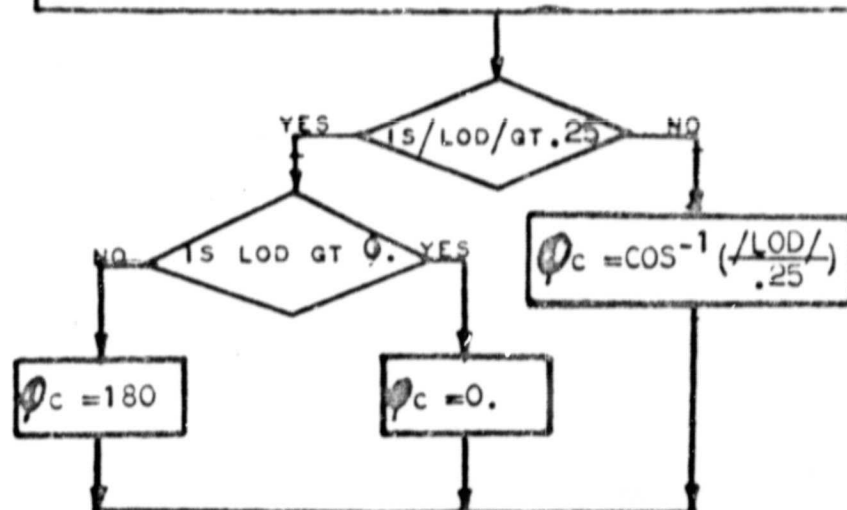


1. CONSTANT-G GUIDANCE EQUATIONS AND LOGIC

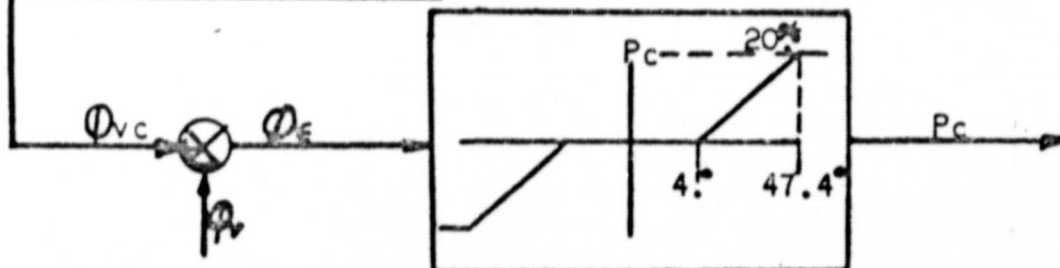
$$APACC = \sqrt{A_x^2 + A_z^2}$$

$$ACACC = \left(\frac{V_T}{663896907} - 1. \right) G$$

$$LOD = \frac{ACACC}{DD} + .01(APACC - DD) - .001(\dot{H} + 57000 \left[\frac{DD}{V_T} \right])$$



2. ROLL RATE COMMAND LOGIC



3. RANGE TO GO EQUATIONS

$$V_i = \int A_x DT + V_i(1c) \quad RTG = \int V_i DT$$

FIGURE 11 ADDITIONAL EQUATIONS USED TO GENERATE EMS RANGE TO GO VALUES FOR CONSTANT-G ENTRY PROFILES.

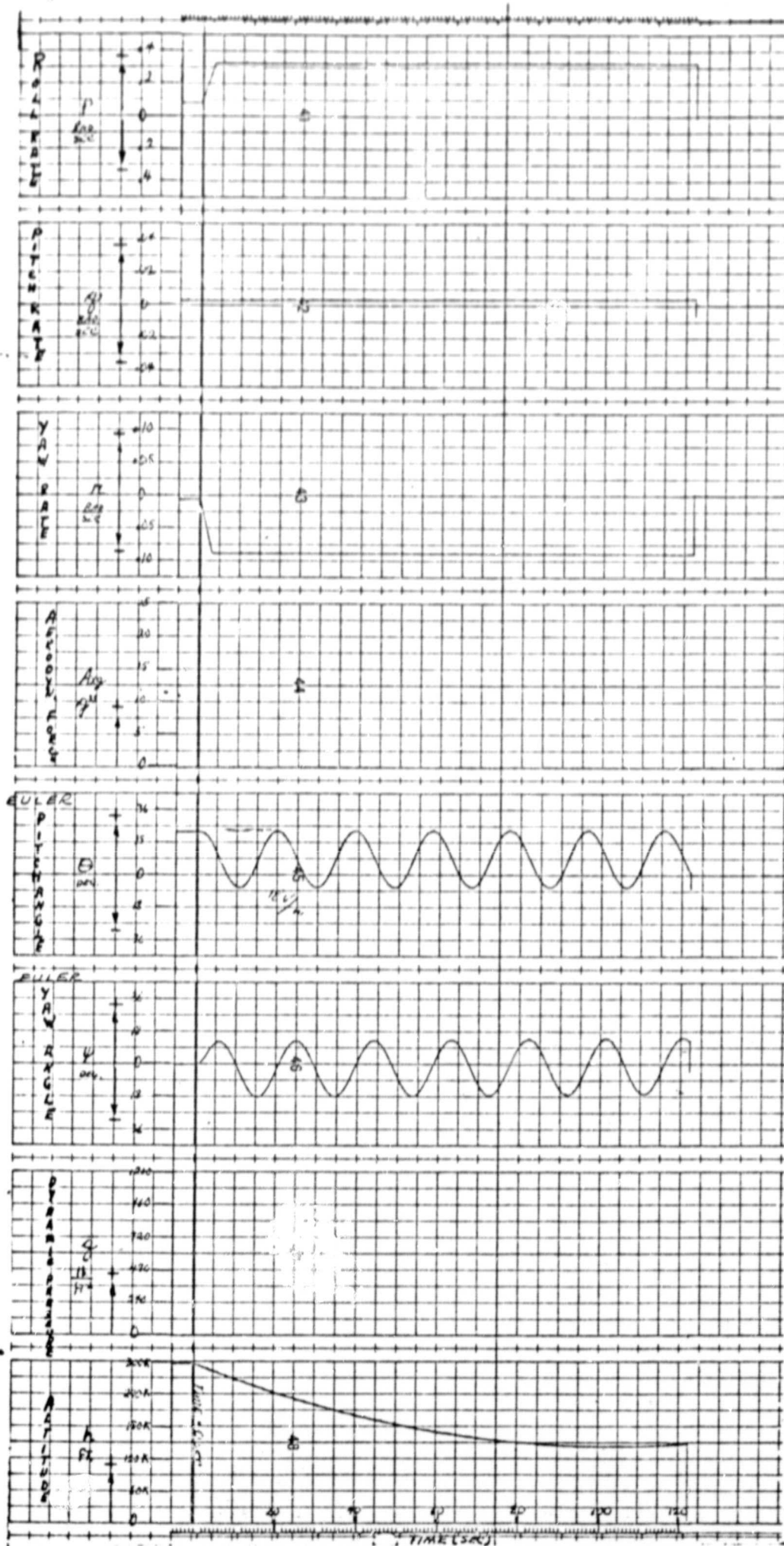


Figure 12 - Dynamic check case 1, rolling entry with no aerodynamics

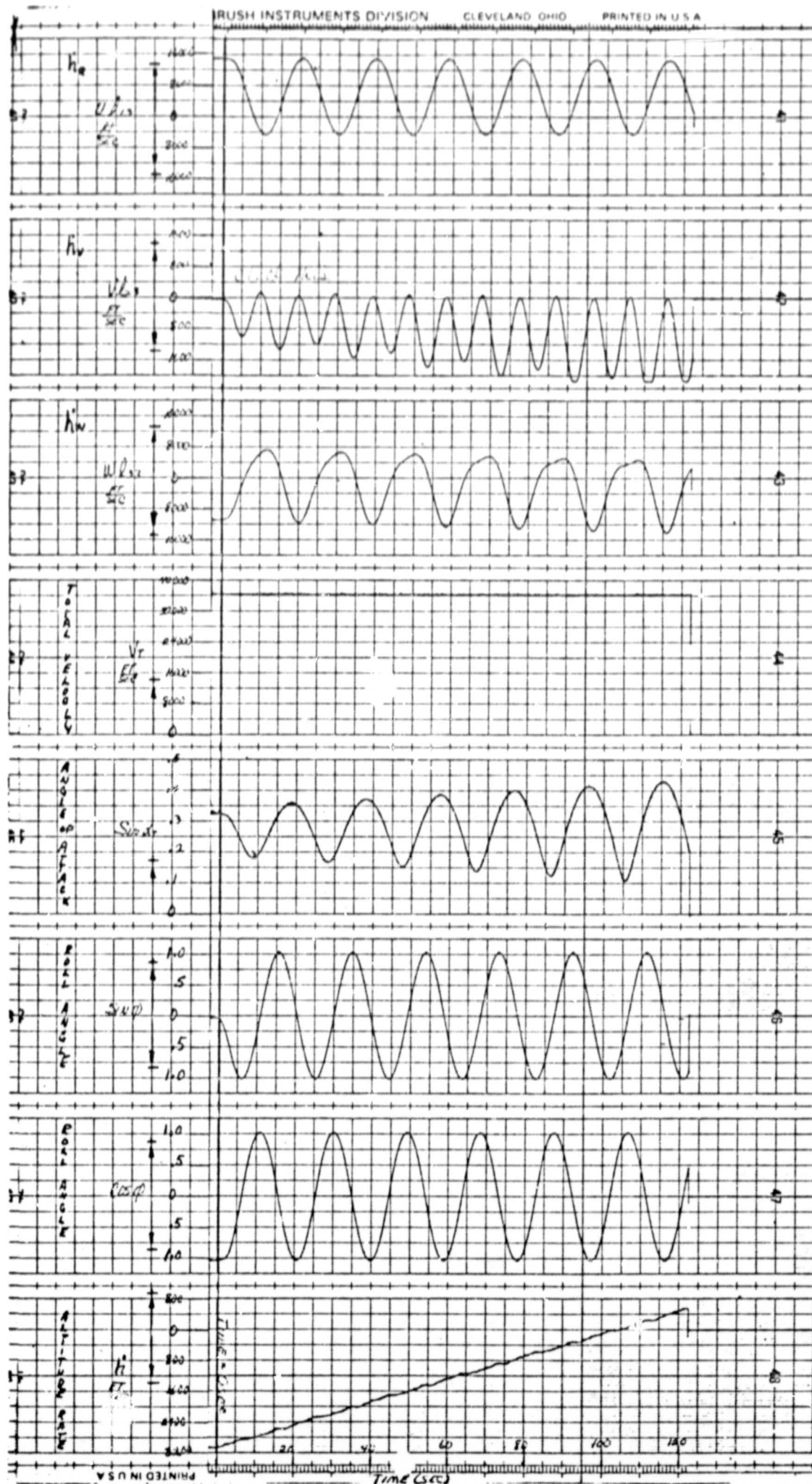


Figure 12 - continued

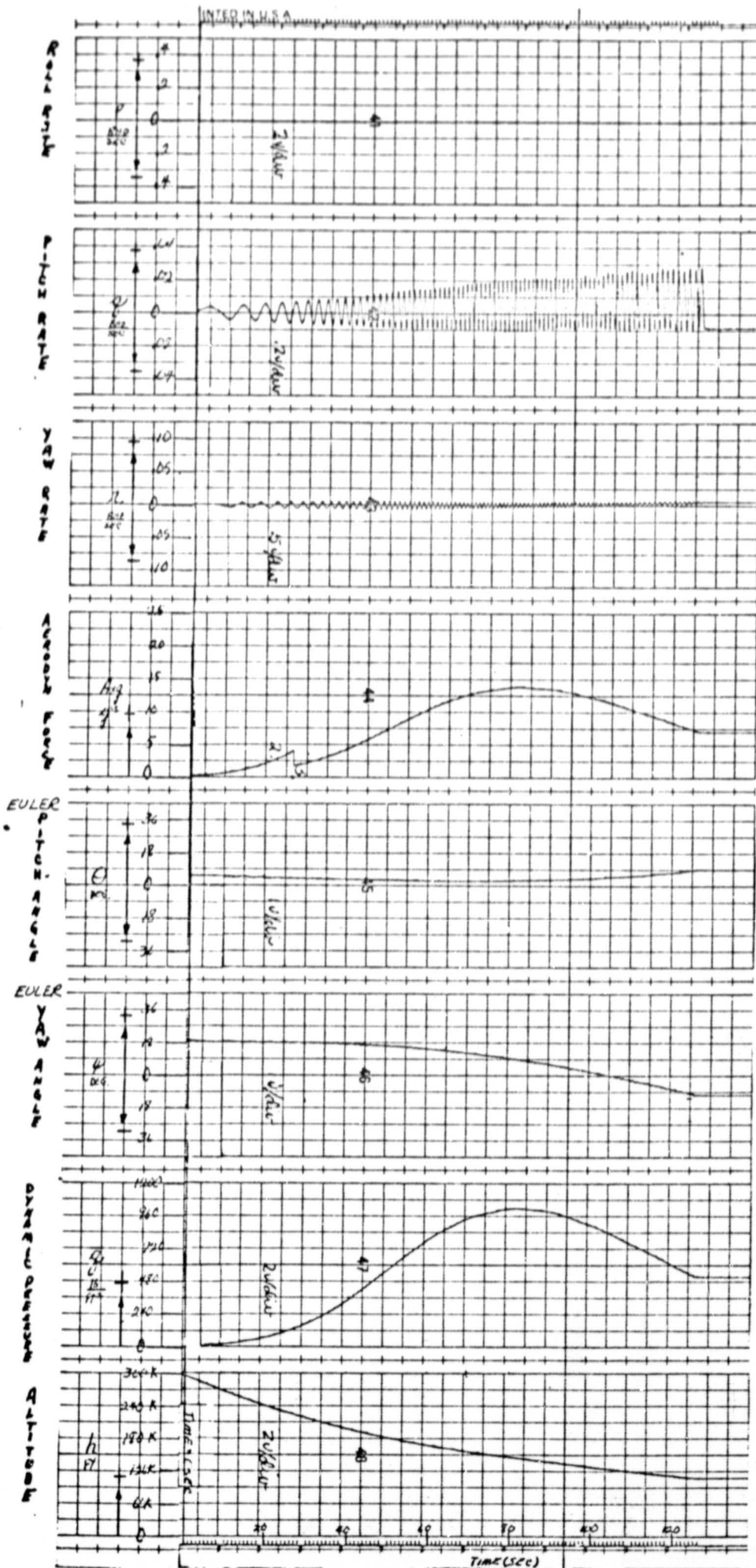


Figure 13 - Dynamic check case 2, constant bank angle ($\phi = -90^\circ$) with aerodynamics

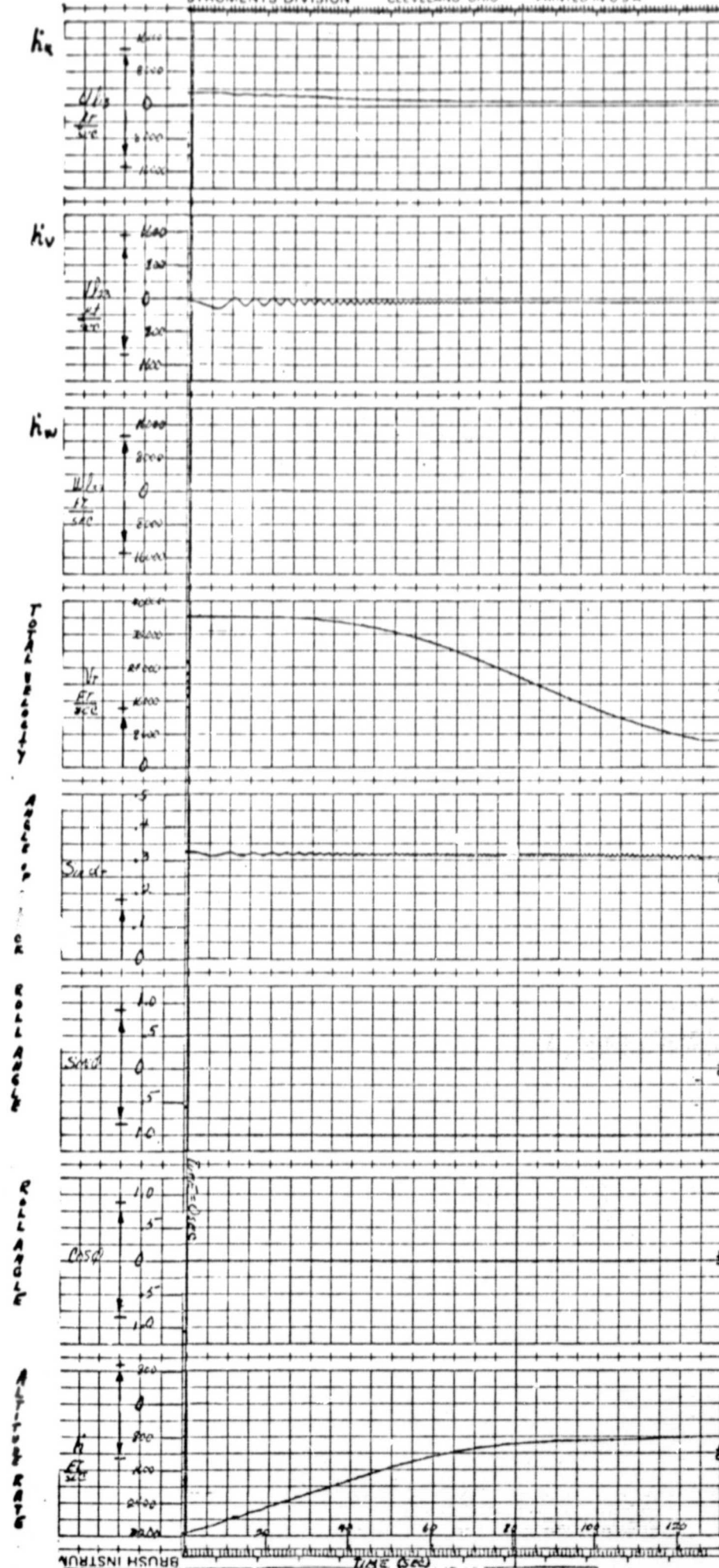


Figure 13 - continued

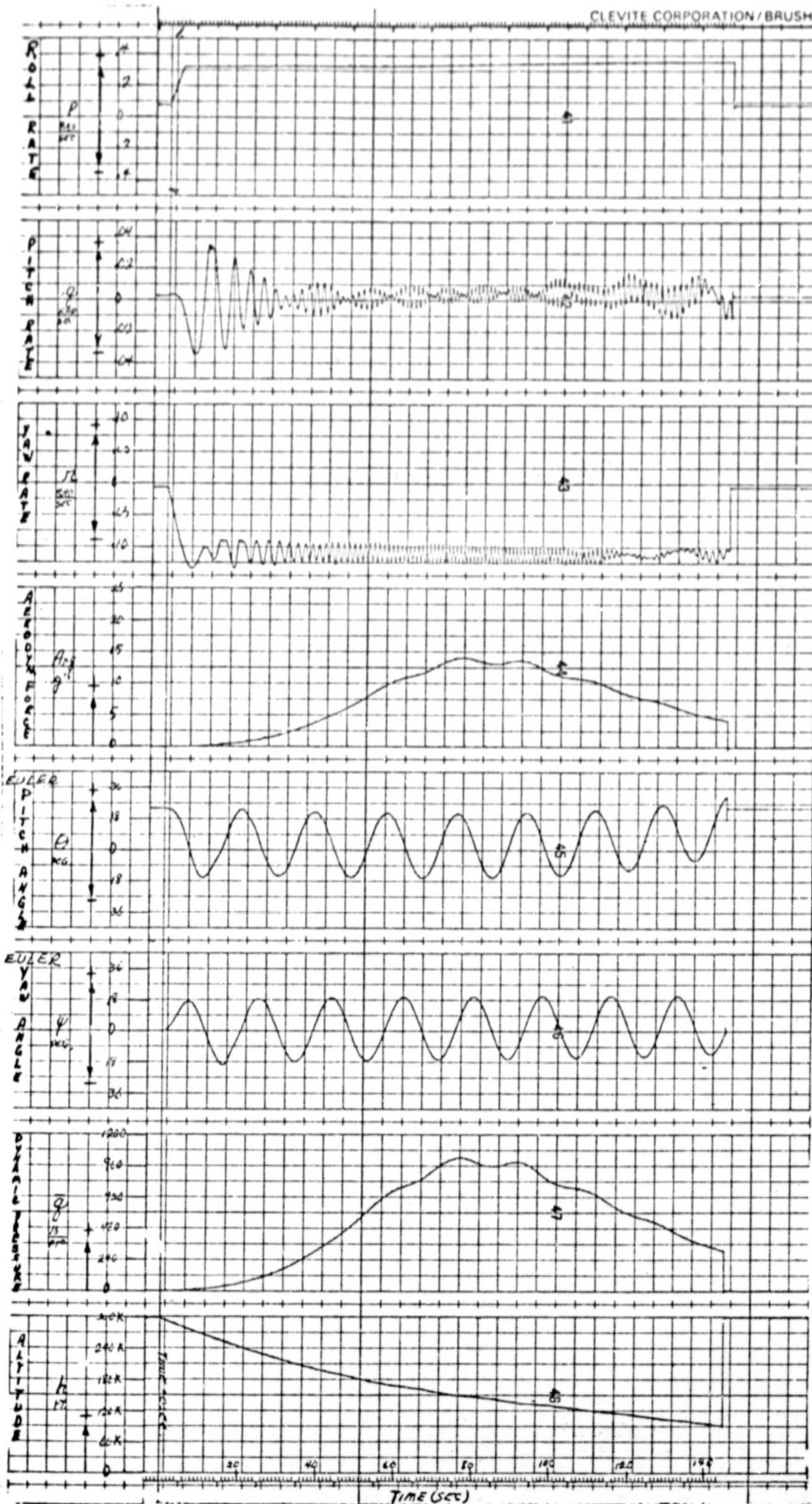


Figure 14 - Dynamic check case 3, continuous 20°/s rolling entry with aerodynamics

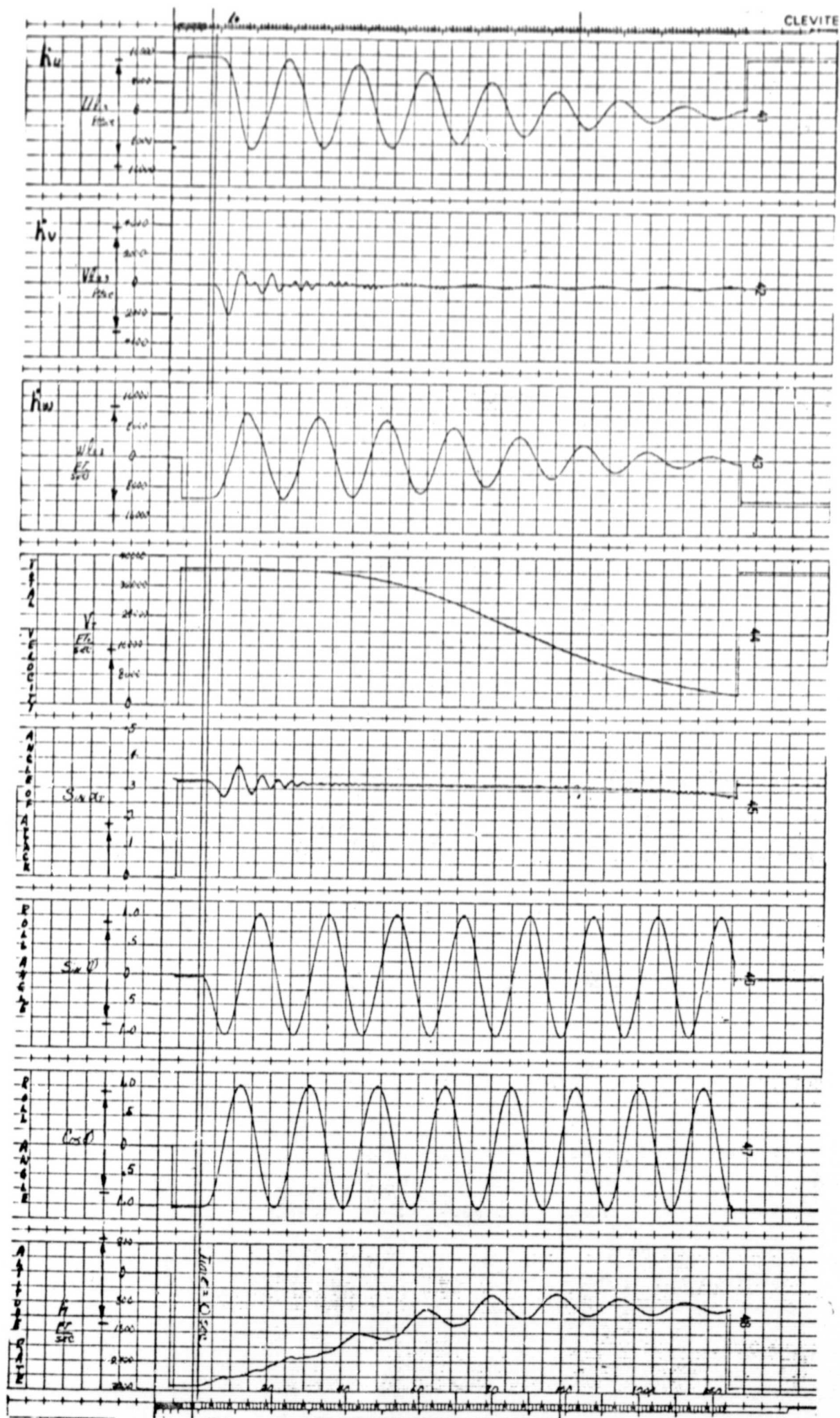


Figure 14 - continued

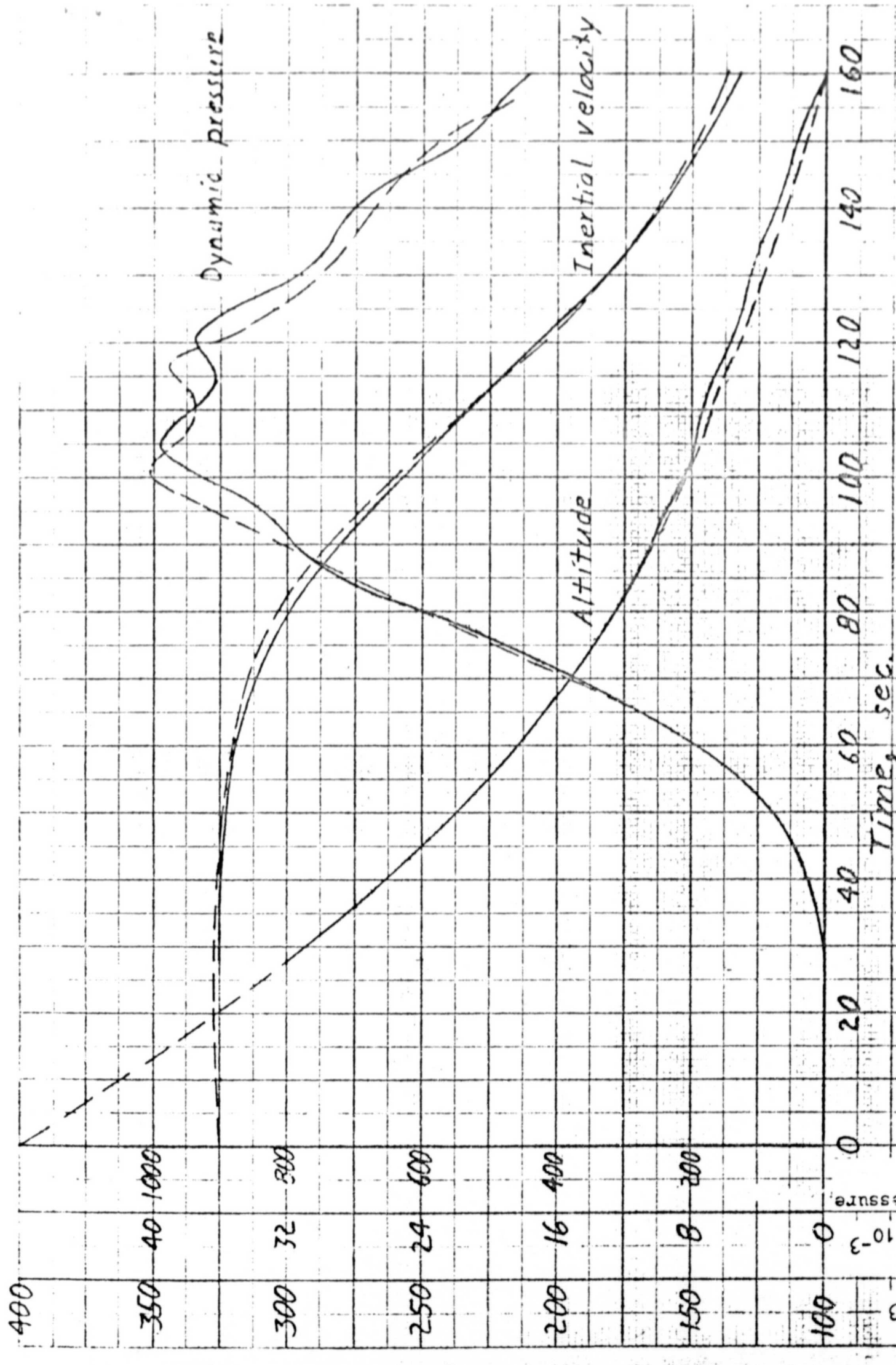


Figure 15- Comparison of analog solution of simplified entry equations with results obtained from the CM Guidance and Control Verification Simulation. Initial conditions correspond to an inertial velocity of 36,100 ft/sec and a flight path angle of -6.4 deg at an altitude of 400,000 feet. The commanded roll rate is 20 deg/sec. $K_1 = 1.06$.